

Autonomous and Self-Adapting System for Synthetic Media Detection and Attribution

Aref Azizpour, Tai D. Nguyen, Matthew C. Stamm
Drexel University
Philadelphia, PA, USA

aa4639,tdn47,mcs382@drexel.edu

Abstract

Rapid advances in generative AI have enabled the creation of highly realistic synthetic images, which, while beneficial in many domains, also pose serious risks in terms of disinformation, fraud, and other malicious applications. Current synthetic image identification systems are typically static, relying on feature representations learned from known generators; as new generative models emerge, these systems suffer from severe performance degradation. In this paper, we introduce the concept of an autonomous self-adaptive synthetic media identification system—one that not only detects synthetic images and attributes them to known sources but also autonomously identifies and incorporates novel generators without human intervention. Our approach leverages an open-set identification strategy with an evolvable embedding space that distinguishes between known and unknown sources. By employing an unsupervised clustering method to aggregate unknown samples into high-confidence clusters and continuously refining its decision boundaries, our system maintains robust detection and attribution performance even as the generative landscape evolves. Extensive experiments demonstrate that our method significantly outperforms existing approaches, marking a crucial step toward universal, adaptable forensic systems in the era of rapidly advancing generative models.

1. Introduction

Rapid advances in artificial intelligence have given rise to powerful generative models capable of producing highly realistic synthetic images. Unfortunately, these generative systems can be misused to facilitate socially harmful activities such as disinformation campaigns, identity theft, social engineering, and fraud. Motivated by the need to detect and mitigate such threats, researchers have developed various techniques to identify synthetic images and attribute them

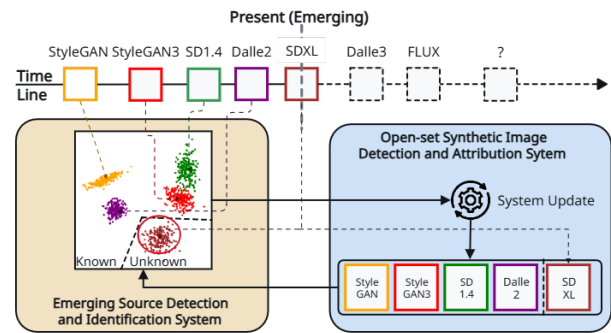


Figure 1. Overview of our autonomous self-adapting synthetic image identification framework. As new generative sources emerge, the system identifies them as unknown, and updates its models accordingly.

to their underlying generators.

Current synthetic image identification systems typically rely on feature representations learned from known generators [9, 18, 26, 39, 44], performing well only when test images originate from these known sources. However, new generative models frequently emerge, often employing novel architectures and creating forensic patterns absent in the training data. Consequently, systems optimized for known sources suffer significant performance degradation on out-of-distribution images, limiting their ability to respond effectively as new threats continually emerge [11, 13, 33].

Transferable [8, 33, 35, 38, 40, 41] and zero-shot detection [14, 32] methods address this limitation by exploiting artifact patterns assumed common across generators. Although initially effective, their performance deteriorates over time as newer generative architectures increasingly differ from previously encountered forensic cues. Because these methods depend on static forensic features derived from a limited training distribution, they fail to adapt continuously, becoming progressively less effective as generative

technologies evolve.

Open-set attribution methods [1, 17, 45] improve detection by differentiating known generators from unknown sources. However, these methods struggle to determine whether unknown images originate from a single emerging source or multiple distinct sources. Additionally, since open-set systems rely on fixed models trained on initial distributions, their performance deteriorates as new generators continually emerge, rendering them ineffective in dynamically evolving environments.

Continual learning methods [4, 28] incrementally update synthetic media identification systems with new data, helping maintain or recover performance. However, these methods require manual data collection, curation, and labeling for each new source, making them slow, resource-intensive, and impractical. Moreover, rapid proliferation of new generators—some intentionally concealed—further limits the scalability and responsiveness of human-dependent continual learning approaches.

Each existing approach addresses only a specific aspect of the broader challenge posed by continuously emerging generative models. Transferable and zero-shot methods initially generalize but degrade over time; open-set methods identify unknown samples but fail to discern individual emerging sources; and continual learning methods rely heavily on impractical human intervention. Consequently, there is a critical need for synthetic media identification systems that autonomously detect the emergence of previously unseen generators, adapt their internal models, and maintain robust detection and attribution performance over time.

In this paper, we introduce the concept of an autonomous self-adaptive synthetic media identification system and propose its first concrete implementation. Our system automatically detects synthetic images, identifies new generative sources, and continuously adapts without human intervention. We employ an open-set identification strategy leveraging an evolvable embedding space to discriminate known sources and detect unknown samples. To autonomously discover new generative sources, we propose an unsupervised clustering method that aggregates unknown samples into high-confidence clusters corresponding to emerging generators. Subsequently, the embedding space and decision boundaries are automatically refined based on these clusters, with each update validated to ensure consistent improvement. Extensive experiments demonstrate our method’s consistently superior detection and attribution accuracy, whereas existing approaches experience significant performance degradation over time.

In summary, our main contributions are:

- We introduce the concept of an autonomous self-adaptive synthetic media identification system, capable of automatically detecting and adapting to newly emerging generative sources without human intervention.

- We propose the first concrete implementation of this concept, combining open-set source identification with an evolvable embedding space to robustly discriminate known sources and detect unknown sources.
- We develop an unsupervised clustering approach that autonomously discovers new generative sources by identifying high-confidence subsets within unknown samples.
- We design an automated update and validation mechanism that continuously refines the embedding space and decision boundaries, ensuring system improvements with each adaptation step.
- We conduct extensive experiments demonstrating that our approach achieves consistently superior detection and attribution performance as new generators continually emerge, while existing methods experience significant degradation over time.

2. Background and Related Work

The rapid rise of generative AI has resulted in highly realistic synthetic images, necessitating advances in the detection and source attribution of AI-generated media. Despite significant progress, most existing methods remain static, assuming that all relevant generative sources are known at training time. Consequently, they often struggle to adapt when they encounter images from novel or unseen generators.

Forensic Microstructures. Extensive prior research has demonstrated that the process by which an image is captured or generated leaves behind distinctive forensic microstructures [11, 25, 26, 42, 47]. Cameras and synthetic image generators each imprint unique patterns on images due to their different methods of forming pixel values. Although these microstructures are not directly observable, various techniques have been developed to estimate them for synthetic image detection [6, 10, 12, 23, 31]. However, while these methods capture model-specific traits, they typically do not address how to adapt when new generative processes with distinct microstructures are introduced.

Supervised and Open-Set Approaches. Supervised detectors, trained on large labeled datasets [4, 8, 27, 39, 44, 46], perform well on data similar to the training set but falter against unseen generators due to distributional shifts [11]. Open-set methods extend these approaches by rejecting images that do not match any known source [17, 32, 45], yet they lack mechanisms to integrate novel sources once deployed.

Zero-Shot Detection. In contrast, zero-shot detection methods aim to identify synthetic images without prior exposure to outputs from specific generators, relying solely on training with real images [14, 32]. By focusing on generalizable features rather than generator-specific artifacts, zero-shot approaches mitigate biases introduced by syn-

thetic training data and offer a promising direction for robust detection. However, these methods still assume a fixed decision framework and do not inherently adapt when new, unseen generative techniques emerge.

Motivation for Self-Adaptive Systems. These limitations highlight the need for self-adaptive forensic systems that can dynamically update their detection and attribution modules as new generative models emerge. Our work builds on these advances, proposing a framework that continuously adapts to an ever-changing generative landscape.

3. Problem Formulation

When a synthetic image identification system is created, it is trained using images made by a set of known generative sources. After this initial training phase, however, new image generators will continue to emerge. Despite this, the system must maintain its performance. Furthermore, we assume that a human will not be available to identify the emergence of a new generative source, collect training data from this source, and use this training data to update the synthetic media identification system. As a result, any measures that the system uses to maintain its performance must be performed autonomously.

For a synthetic image identification system to maintain high performance as new generators emerge, it must continuously update itself. To achieve successful autonomous updating, the system must:

1. Detect synthetic images—including those produced by previously unseen generators. This requires the system to have strong transferability or zero-shot detection capabilities.
2. Attribute synthetic media to their correct source or flag them as originating from a new, unknown source.
3. Identify the emergence of a new generator by analyzing data labeled as unknown for self-similar forensic microstructures.
4. Update its detection and attribution models accordingly.

4. Proposed Approach

At a high level, our autonomous self-adapting synthetic media identification system first establishes an open-set framework capable of detecting synthetic images and attributing them to known generators. It then collects images flagged as originating from unknown sources into a buffer. Images in this buffer are clustered to identify potential new generative sources, and the cluster with the highest confidence is designated as a newly discovered generator. Finally, images from this newly discovered generator are used to update and refine the underlying open-set system. This iterative process allows our approach to autonomously adapt to continuously emerging image generators while maintaining robust detection and attribution performance. An overview of our sys-

tem is presented in Fig. 2.

4.1. Open-Set Detection & Source Attribution

We begin by establishing an open-set synthetic media identification system capable of both detection and attribution. This system is initialized at update step $\ell = 0$ and incrementally updated as new generative sources are discovered. At each update step ℓ , the system operates over a set of known synthetic media sources, denoted $S^{(\ell)}$, and an associated training dataset, $\mathcal{D}_T^{(\ell)}$.

As an open-set framework, our system is explicitly designed to detect synthetic images—including those originating from previously unseen sources—and either attribute them to a known source in $S^{(\ell)}$ or label them as unknown (s^u). Throughout this section, we assume that $\mathcal{D}_T^{(\ell)}$ consists of a labeled set of Forensic Self-Descriptions (FSDs) [32], each capture the underlying forensic microstructures of an image.

Capturing Forensic Microstructures. To accurately model the microstructures present in an image, we leverage a recent approach called Forensic Self-Description (FSD). FSDs are learned in a self-supervised manner and have shown strong zero-shot detection and open-set source attribution capabilities. To construct the FSD, a series of predictive filters are applied to produce residuals that emphasize microstructures while suppressing scene content. A multi-scale parametric model is then used to characterize the statistical relationships among these residuals, and the resulting model parameters, denoted by ϕ , serve as the FSD of the image.

Enhanced Source Separation Embedding Space. As demonstrated by Nguyen et al. [32], while FSDs provide very robust zero-shot detection capabilities, they are not explicitly optimized to accurately discriminate between different synthetic sources.

To address this limitation, we propose learning an enhanced embedding space that more effectively separates image sources. To do this, we must design our embedding space such that: (1) Embeddings from a common source must be close together; (2) Embeddings from different sources must be far apart; and (3) All aspects of the forensic microstructures must be preserved to retain strong detection capabilities.

To achieve these goals, first, let the FSD be denoted as ϕ_k and a new projection at time step ℓ be $f^{(\ell)}$ such that $\psi_k = f^{(\ell)}(\phi_k)$, where ψ_k is an enhanced embedding. We can attain goals (1) and (2) by training $f^{(\ell)}$ with a loss function as follows:

$$\mathcal{L}_{\text{att}} = \sum_{\mathcal{T}_j \in \mathcal{T}} \left[\|f^{(\ell)}(\phi_j^a) - f^{(\ell)}(\phi_j^p)\|_2^2 - \|f^{(\ell)}(\phi_j^a) - f^{(\ell)}(\phi_j^n)\|_2^2 + m \right]_+, \quad (1)$$

where $[\cdot]_+$ denotes $\max(0, \cdot)$, \mathcal{T}_j is a triplet consisting of $(\phi_j^a, \phi_j^p, \phi_j^n)$, and m is the margin enforced between positive

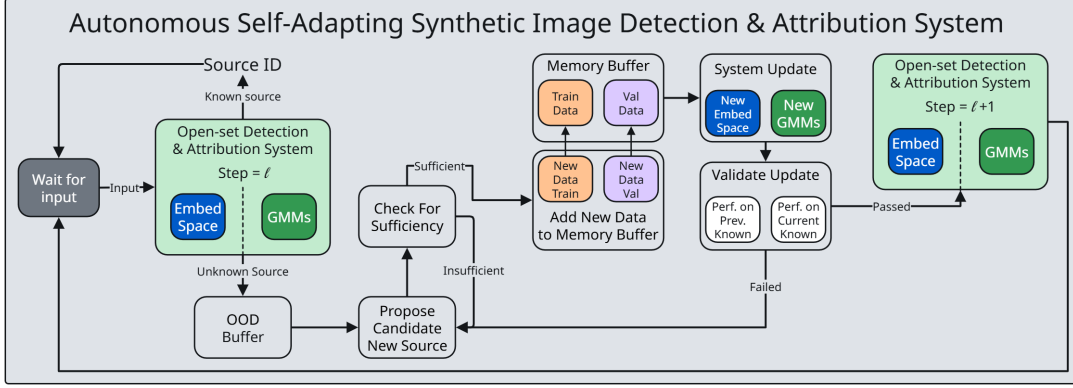


Figure 2. System diagram of our proposed self-adaptive forensic framework, which continuously identifies and buffers unknown samples, clusters them to discover emerging sources, and updates the embedding space and open-set model as needed.

(same sources) and negative (different sources) pairs.

To fulfill goal (3) of retaining all aspects of the forensic microstructures, we design a reconstruction function g that decodes the projected enhanced embedding ψ_k back into the FSD space. If $g(\psi_k) = \hat{\phi}_k \approx \phi_k$, then ψ_k should preserve the original FSD with minimal distortion. Hence, we define our forensic microstructures preservation loss as:

$$\mathcal{L}_{\text{pres}} = \|\phi_k - g(f^{(\ell)}(\phi_k))\|_2^2, \quad (2)$$

and, the total embedding loss is then calculated as:

$$\mathcal{L}_{\text{embed}} = \mathcal{L}_{\text{att}} + \lambda \mathcal{L}_{\text{pres}}, \quad (3)$$

where λ is a hyperparameter that balances the contribution of the preservation loss relative to the attribution loss.

Fig. 3 shows 2D t-SNE [43] plots comparing the original FSD space and our enhanced embedding space, demonstrating improved separability among sources. Notably, real images (labeled 0 in the blue cluster) remain well separated from generative sources, preserving detection capability while enhancing discrimination.

Detecting and Attributing Image Sources. After obtaining our enhanced embeddings, we use them to perform open set synthetic image detection and source attribution. To accomplish this, we first build a model of the distribution of embeddings from each known source. Here, we model each of these distributions using a Gaussian mixture model such that $p(\psi_k | s) = \text{GMM}(\psi_k | \{\pi_{s,i}, \mu_{s,i}, \Sigma_{s,i}\}_{i=1}^{M_s})$, where M_s is the number of mixture components for source s , and $\pi_{s,i}$, $\mu_{s,i}$, and $\Sigma_{s,i}$ represent the mixture weights, means, and covariance matrices, respectively.

At test time, for each new image x_k with embedding ψ_k , the system computes $p(\psi_k | s)$ for every $s \in \mathcal{S}^{(\ell)}$ using the learned GMMs. We then define the candidate source s^c as:

$$s^c = \arg \max_{s \in \mathcal{S}^{(\ell)}} p(\psi_k | s). \quad (4)$$

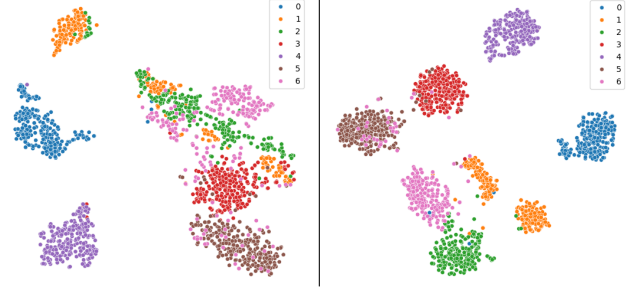


Figure 3. 2D t-SNE plot of the embedding space before and after applying the enhanced source separation projection.

Subsequently, we define the attribution function $\alpha(\psi_k)$ by applying a confidence threshold τ_{reject} :

$$\alpha(\psi_k) = \begin{cases} s^c & \text{if } p(\psi_k | s^c) > \tau_{\text{reject}}, \\ s^u & \text{otherwise.} \end{cases} \quad (5)$$

Here, $s^u \notin \mathcal{S}^{(\ell)}$ denotes the "unknown" source.

We then collect and store unknown examples in a buffer \mathcal{B} for later analysis and identification of a potential new source.

4.2. New Source Discovery

Periodically, the buffer is analyzed by a dedicated subsystem designed to detect the emergence of new generative sources. When a new source appears, a significant portion of the buffered data exhibits similar forensic microstructures. To identify these, we apply a clustering algorithm that groups the enhanced embeddings based on their forensic patterns. This process yields a set of clusters \mathcal{C} such that

$$\mathcal{C} = \{C_1, C_2, \dots, C_m\}, \quad \text{with } |C_1| \geq |C_2| \geq \dots \geq |C_m|,$$

where $|\cdot|$ denotes the set cardinality operator.

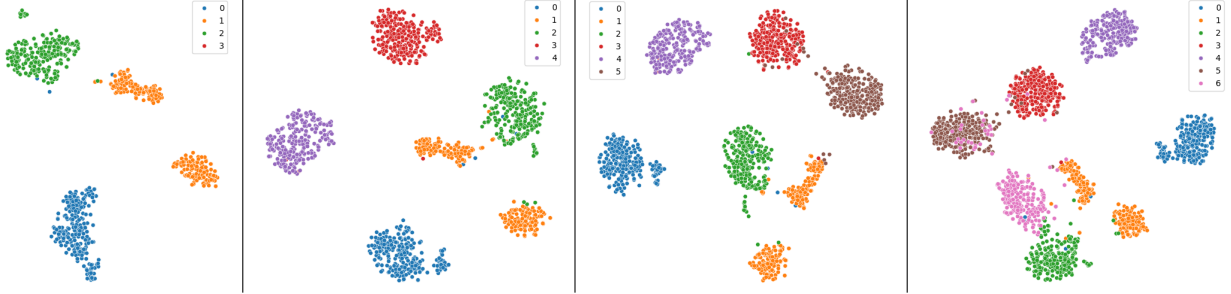


Figure 4. 2D t-SNE plots of the embedding space after updating at time step 0, 1, 2, and 3 (from left to right).

To select a candidate cluster from \mathcal{C} that may correspond to a new source, we begin with the cluster containing the most elements, denoted C^* . To confirm that C^* represents a coherent, novel source, we perform a sufficiency check: C^* is deemed sufficient if $|C^*| > \tau_s$; otherwise, it is rejected.

If C^* passes this test, we conclude that a new source has been identified and proceed to update the detection and attribution subsystem. If not, no new source is discovered, and the system continues operating while awaiting additional data in the buffer.

4.3. System Update

Once a new source, denoted as s_n , is discovered, we update our set of known sources as follows:

$$\mathcal{S}^{(\ell+1)} = \mathcal{S}^{(\ell)} \cup \{s_n\}. \quad (6)$$

We then partition the candidate cluster C^* into training (C_T^*) and validation (C_V^*) subsets, which are merged with our existing training and validation sets:

$$\mathcal{D}_T^{(\ell+1)} = \mathcal{D}_T^{(\ell)} \cup C_T^* \quad \text{and} \quad \mathcal{D}_V^{(\ell+1)} = \mathcal{D}_V^{(\ell)} \cup C_V^*. \quad (7)$$

Next, we update the source separation embedding space using $\mathcal{D}_T^{(\ell+1)}$ via the process and loss defined in Eq. 3 (see Sec. 4.1). Finally, our open-set detection and attribution system is updated by training new GMMs for each source in $\mathcal{S}^{(\ell+1)}$.

4.4. Validating System Update

Depending on the data introduced, the selected candidate cluster may sometimes consist of out-of-distribution data from known sources rather than a genuinely emerging generative source. Updating the system with such a cluster can lead to a significant drop in performance.

To mitigate this risk, we validate each update using the validation data $\mathcal{D}_V^{(\ell+1)}$. The underlying premise is that a valid update should not degrade performance on previously known sources and must achieve sufficiently high performance on the new source. Specifically, we measure: (1) detection accuracy on the previously known sources $\mathcal{S}^{(\ell)}$,

(2) source attribution accuracy on $\mathcal{S}^{(\ell)}$, and (3) source attribution accuracy on the new source.

If the update meets all three criteria, it is accepted. Otherwise, we first attempt to select a different candidate cluster from \mathcal{C} ; if that fails, we adjust the clustering hyperparameters and try again. Should these attempts prove unsuccessful, the system reverts to normal operation and waits for additional data.

5. Experiments and Results

Implementation Details. We train our embedding model using AdamW [24] (10^{-4} learning rate, 0.01 weight decay) with mini-batches of 256 samples and 64 hardest positives/negatives per anchor. The embeddings are modeled using GMMs [29] with a confidence threshold set to maximize TPR – FPR. For clustering, we employ DBSCAN [16] with a minimum sample size 7 and epsilon searched between 5 and 20. Additional implementation details are provided in the supplemental materials.

Datasets. To conduct our experiments, we used publicly available datasets containing both real and synthetic images. For real images, we use ImageNet-1k [37]. For synthetic images, we gather images generated by StyleGAN [1-3] [20–22], ProGAN [19], DALLE3 [7], Midjourney v6 [30], Adobe Firefly [2], Stable Diffusion (SD) 1.4 [36], SD 1.5 [36], SD 3.0 [15], and SDXL [34]. These images are collected from the OSSIA dataset [17], and the Synthbuster dataset [5]. More details about these datasets are provided in the supplemental materials.

Data Setup. To construct our autonomous self-adapting system, we first initialize the open-set source identification module using a reserved data subset containing training examples from several initially known sources. Next, to introduce our system to data from new sources, we create an “observation” subset that is disjoint from the initial set and includes images drawn from both previously known sources and new sources. Once the system has observed data from a new source, we evaluate its detection and attribution capabilities using an exclusive test subset. These three data partitions enable us to rigorously assess how effectively the

Type	Method	Initial			Average over each new source			Final		
		Det. Acc.	AUC%	Att. Acc.	Det. Acc.	AUC%	Att. Acc.	Det. Acc.	AUC%	Att. Acc.
Det.	CNNDet [44]	83.9	95.2	-	58.2	65.7	-	65.2	73.8	-
	UFD [33]	78.7	93.6	-	64.8	77.4	-	68.6	81.8	-
	NPR [41]	91.6	97.5	-	82.1	85.1	-	84.7	88.5	-
	ZED [14]	64.6	65.5	-	56.2	54.7	-	58.5	57.7	-
OS Att.	Fang et al. [17]	98.7	99.8	99.0	69.3	89.5	0.0	77.3	92.3	33.0
	POSE [45]	95.8	99.3	88.0	49.4	45.7	0.0	60.0	58.1	29.3
	FSD [32]	89.1	98.8	71.1	85.2	97.3	0.0	86.3	97.7	23.7
SA	Ours	99.5	99.9	99.5	98.4	97.6	85.3	97.8	98.3	83.0

Table 1. Comparison of detection and source attribution performance. The table reports detection accuracy, AUC, and source attribution accuracy initially, on newly introduced sources (averaged), and overall performance after all sources are integrated. Our proposed self-adaptive (SA) framework consistently outperforms both detection-only and static open-set attribution methods, demonstrating robust continuous detection and superior attribution on emerging generative models.

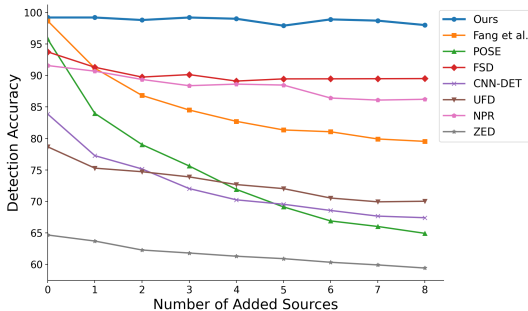


Figure 5. Evolution of detection accuracy as new generative sources are introduced sequentially. Our self-adaptive approach (blue line) maintains high accuracy.

system adapts to emerging sources while maintaining robust performance on known ones.

5.1. Sequentially Adapting to Multiple New Sources

In this section, we conducted an experiment to evaluate our system’s performance in a real-world setting where new synthetic sources continuously emerge. To accomplish this, periodically, we exposed our system to both images from the known sources and images from one newly emerging source using an observation subset. At time step $\ell = 0$, the system is initialized with a reserved subset containing real images from ImageNet-1K and synthetic images from StyleGAN [1–3]. After the new source was introduced, we then measured the system’s detection and attribution performance.

Metrics. We report detection performance using accuracy and the Area Under the ROC Curve (AUC) metrics. We also report source attribution performance using accuracy. While all metrics are measured after each step, we average each metric over time to provide aggregated results.

Competing Methods. To compare our system’s performance at detecting synthetic images, we selected four state-

Metric	Emerging Sources								Avg.
	Progan	Dalle3	MJv6	Firefly	SD1.4	SD1.5	SD3	SDXL	
Det. Acc.	95.9	98.4	99.1	99.2	97.1	98.5	99.2	92.1	97.4
Det. AUC%	99.9	99.9	98.7	98.1	98.7	96.5	99.6	90.0	97.7
Att. Acc.	92.4	83.6	94.0	67.6	49.6	90.8	79.2	82.0	79.9

Table 2. Detection and attribution performance for individual emerging generators.

of-the-art methods: CNNDet [44], UFD [33], NPR [33], and ZED [14]. Additionally, to assess source attribution performance, we compared our system to three best performing open-set methods: Fang et al. [17], POSE [45], and FSD [32].

Results. The results of this experiment are presented in Tab. 1. These findings show that our system achieves the highest detection and attribution performance at the final evaluation, experiencing only a minor decrease from its initial performance. In contrast, competing methods all experience significant performance drop over time. In particular, Tab. 1 indicates that our final detection accuracy reaches 97.8%, surpassing all other methods by a large margin. This trend is further illustrated in Fig. 5, where our system’s detection accuracy remains consistently high at each time step, in contrast to the gradual decline observed for other approaches. Likewise, Fig. 6 shows that while our method’s source attribution accuracy decreases slightly over time, its final performance of 83% is still 2.5 times higher than that of the next-best method, 33%. This is because existing approaches cannot update themselves to include new sources when performing attribution.

We note that while FSD’s detection and attribution performance declines over time, our system maintains consistently high performance. This indicates that our superior results are not due to FSD’s inherent strengths, but rather our system’s capability to self-adapt. Specifically, our system continuously evolves its embedding space in response to newly introduced data, thereby enabling more accurate

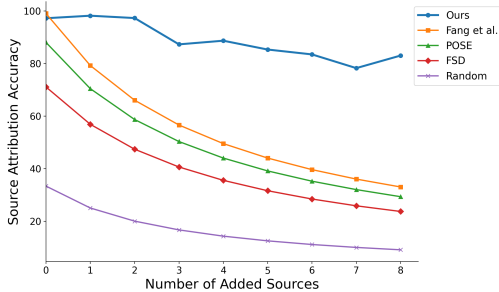


Figure 6. Evolution of source attribution as new generative sources are introduced sequentially. Our self-adaptive approach (blue line) maintains high accuracy, with minimal performance drop.

detection and source attribution.

Another key insight from these experiments is that some competing methods maintain reasonably high final AUC yet suffer considerable decreases in detection accuracy from their initial deployment. For example, Fang et al. retains a final AUC of 92.3%, but its detection accuracy drops from 98.7% initially to 77.3%. This occurs because these approaches primarily rely on thresholds determined at initial deployment, which cannot be updated without human intervention. Consequently, despite retaining high theoretical potential as indicated by AUC, their practical performance sharply declines as novel sources emerge, highlighting their inability to autonomously adapt in real-world conditions.

5.2. Adapting to Individual New Sources

While the previous experiment evaluated average performance across many newly emerging sources, we now present a more granular analysis by measuring our system’s ability to adapt to a single, individual new source. To do this, we initialize our system similar to Sec. 5.1, introduce it to one emerging source and measure its detection and attribution performance without allowing any validation step after the update. We proceed to repeat this process for all eight sources in our dataset and report detailed performance metrics in Tab. 2.

Results. The results of this experiment are presented in Tab. 2. These findings show that our system achieves uniformly high detection performance, with detection accuracy above 92% for every newly introduced generator. Likewise, the average detection AUC exceeds 97%, indicating robust real-versus-synthetic discrimination across diverse generative models. By contrast, attribution performance, though generally strong, does decline for certain generators (Firefly, SD1.4, SD3), dipping below 80% accuracy. This occurs primarily because some new sources naturally exhibit forensic microstructures that closely resemble at least one known source. Consequently, images from known sources can contaminate the cluster of the newly emerg-

Component	Method	Det. Acc	Att. Acc.
	Proposed		98.0
Cluster. Alg.	k-means	87.9	46.1
Embd. Spac.	No Preservation	95.2	47.0
	Overly Preserved	96.0	42.2
Val. Crit.	No Validate	92.7	49.9
	No New Crit.	97.9	60.1
	No Det. Crit.	96.6	45.4
	No Att. Crit.	95.0	51.9

Table 3. Results of ablation study of our proposed method: Comparison of different design choices.

ing source, thereby diminishing attribution accuracy for the newly emerged source. While we can still reliably detect these synthetic sources, it is more challenging to correctly attribute them without perfectly labeled data.

5.3. Ablation Study

We conducted an ablation study to assess the impact of various design choices on the final performance of our proposed method. In this study, we repeated the experiment described in Sec. 5.1 while varying key parameters across three components: the clustering algorithm, the embedding space (controlled by the balance factor λ), and the validation criteria. The ablation results are provided in Tab. 3.

Clustering Algorithm. We evaluated the effect of replacing our chosen clustering algorithm, DBSCAN, with an alternative method (k-means [3]). The results in Tab. 3 clearly indicate that using k-means leads to significant drops in both detection and attribution performance. This finding highlights the critical role of our clustering approach in effectively isolating emerging sources.

Embedding Space. We investigated the influence of different values for the balance factor λ in our enhanced source separation embedding space. As shown in Tab. 3, when λ is set to 0.0, meaning no preservation loss term, the system experiences a significant drop in terms of detection accuracy. In contrast, introducing an overly preserved $\lambda = 5.0$ leads to a noticeable drop in detection and source attribution accuracy. This suggests that this weight must be set correctly to balance between the two competing loss terms.

Validation Criteria. We further analyzed the impact of the validation criteria by individually omitting each condition from our set of requirements. The results in Tab. 3 show that the removal of any single validation criterion leads to noticeable performance degradation, underscoring the necessity of each component for maintaining robust overall performance.

6. Discussion

Enhanced Separation Embedding Space. The results comparing different variants of our embedding space loss

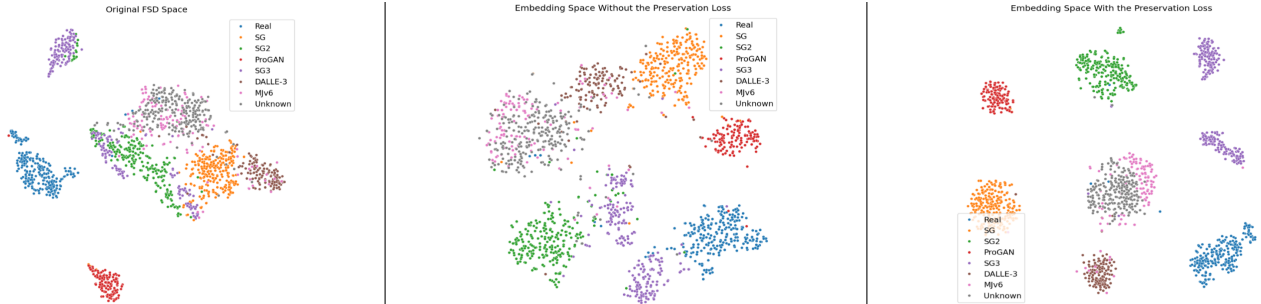


Figure 7. 2D t-SNE plots of the original FSD space (left), enhanced separation embedding space with preservation loss term (right), and without this term (middle).

function (Eq. 3) are shown in Tab. 4 and illustrated in Fig. 7. We examine three embedding configurations: the original native FSD embedding space, enhancement using only the contrastive loss term, and enhancement using both contrastive and preservation loss terms. The original FSD embedding clearly distinguishes real images from synthetic ones but struggles to differentiate among multiple synthetic sources. Introducing the contrastive loss significantly improves the separation between synthetic sources, increasing detection accuracy to 98.1% and attribution accuracy to 99.8%. However, robust rejection of unknown sources (AU-CRR: 59.5%→61.9%) remains limited without the preservation term. Incorporating both contrastive and preservation terms leads to the best overall performance (64.2% AU-CRR), highlighting that the preservation loss is crucial for maintaining robust and balanced performance in open-set detection and attribution tasks.

Continuously Evolving Embedding Space. The evolution of our embedding space over successive update steps is illustrated in Fig. 4. Initially, the embedding space separates known sources into distinct, well-defined clusters. As new generative sources emerge at each subsequent update step, our system automatically integrates these sources by refining its embedding representation, clearly illustrated by the progressive addition of well-separated clusters. Notably, each incremental update effectively accommodates the newly discovered source without disrupting existing embeddings, highlighting the stability of our adaptation approach. This continuous evolution of the embedding space allows our system to robustly distinguish among multiple emerging sources, sustaining high detection and attribution accuracy over time, even as the landscape of generative models becomes increasingly complex.

Limitations & Future Work. Our autonomous self-adaptive synthetic media identification system while strong, can still face certain limitations. In particular, our approach relies on unsupervised clustering to identify emerging sources, which may occasionally group together distinct sources sharing similar forensic patterns. Additionally, while the embedding space evolves continuously, per-

Embedding Space	Det. Acc.	Det. AUC%	Att. Acc.	AU-CRR	AU-OSCR
FSDs only	92.4	96.3	90.7	59.5	56.0
No Preservation	98.1	99.6	99.8	61.9	61.9
Contrastive+Preservation	99.5	99.9	99.5	64.2	64.2

Table 4. Embedding space selection. Our approach with preservation loss outperforms FSDs and an embedding space without the preservation loss in detection and source attribution accuracy, and open-set metrics.

formance improvements depend on the quality and representativeness of the identified subsets used for updates. Future work could explore semi-supervised clustering or advanced uncertainty estimation methods to further improve the separation of closely related novel sources. Furthermore, incorporating active learning strategies or weak supervision signals could enhance the reliability of updates, thereby strengthening the system’s robustness in highly dynamic, real-world scenarios.

7. Conclusion

We presented an autonomous, self-adaptive synthetic media identification system that dynamically detects synthetic images, attributes them to known sources, and—crucially—adapts to emerging generative models without human intervention. Our approach combines open-set identification with an evolving embedding space, an unsupervised clustering mechanism to discover novel generators, and an automated update and validation process that continuously refines detection and attribution performance. Extensive experiments demonstrate that our system consistently outperforms static methods, maintaining high detection accuracy and robust source attribution even as new generators emerge.

References

- [1] Lydia Abady, Jun Wang, Benedetta Tondi, and Mauro Barni. A siamese-based verification system for open-set architecture attribution of synthetic images. *Pattern Recognition Letters*, 180:75–81, 2024. 2
- [2] Adobe. Adobe Firefly. <https://www.adobe.com/>

- [products/firefly.html](#). Accessed: March 7, 2025. 5
- [3] David Arthur and Sergei Vassilvitskii. k-means++: The advantages of careful seeding. Technical report, Stanford, 2006. 7
- [4] Aref Azizpour, Tai D. Nguyen, Manil Shrestha, Kaidi Xu, Edward Kim, and Matthew C. Stamm. E3: Ensemble of expert embedders for adapting synthetic image detectors to new generators using limited data. In *Proceedings of the IEEE/CVF Conference on Computer Vision and Pattern Recognition (CVPR) Workshops*, pages 4334–4344, 2024. 2
- [5] Quentin Bamme. Synhbuster: Towards detection of diffusion model generated images. *IEEE Open Journal of Signal Processing*, 5:1–9, 2024. 5
- [6] Mauro Barni, Kassem Kallas, Ehsan Nowroozi, and Benedetta Tondi. Cnn detection of gan-generated face images based on cross-band co-occurrences analysis. In *2020 IEEE International Workshop on Information Forensics and Security (WIFS)*, pages 1–6, 2020. 2
- [7] James Betker, Gabriel Goh, Li Jing, Tim Brooks, Jianfeng Wang, Linjie Li, Long Ouyang, Juntang Zhuang, Joyce Lee, Yufei Guo, et al. Improving image generation with better captions. *Computer Science*. <https://cdn.openai.com/papers/dall-e-3.pdf>, 2(3):8, 2023. 5
- [8] Tu Bui, Ning Yu, and John Collomosse. Repmix: Representation mixing for robust attribution of synthesized images. In *European Conference on Computer Vision*, pages 146–163. Springer, 2022. 1, 2
- [9] Lucy Chai, David Bau, Ser-Nam Lim, and Phillip Isola. What makes fake images detectable? understanding properties that generalize. In *European Conference on Computer Vision*, pages 103–120. Springer, 2020. 1
- [10] Umur Aybars Ciftci, Ilke Demir, and Lijun Yin. Fakecatcher: Detection of synthetic portrait videos using biological signals. *IEEE Transactions on Pattern Analysis and Machine Intelligence*, pages 1–1, 2020. 2
- [11] Riccardo Corvi, Davide Cozzolino, Giada Zingarini, Giovanni Poggi, Koki Nagano, and Luisa Verdoliva. On the detection of synthetic images generated by diffusion models. In *ICASSP 2023-2023 IEEE International Conference on Acoustics, Speech and Signal Processing (ICASSP)*, pages 1–5. IEEE, 2023. 1, 2
- [12] Davide Cozzolino, Diego Gagnaniello, and Luisa Verdoliva. Image forgery detection through residual-based local descriptors and block-matching. In *2014 IEEE International Conference on Image Processing (ICIP)*, pages 5297–5301, 2014. 2
- [13] Davide Cozzolino, Giovanni Poggi, Riccardo Corvi, Matthias Nießner, and Luisa Verdoliva. Raising the bar of ai-generated image detection with clip. In *Proceedings of the IEEE/CVF Conference on Computer Vision and Pattern Recognition (CVPR) Workshops*, pages 4356–4366, 2024. 1
- [14] Davide Cozzolino, Giovanni Poggi, Matthias Nießner, and Luisa Verdoliva. Zero-shot detection of ai-generated images. In *European Conference on Computer Vision*, pages 54–72. Springer, 2025. 1, 2, 6
- [15] Patrick Esser, Sumith Kulal, Andreas Blattmann, Rahim Entezari, Jonas Müller, Harry Saini, Yam Levi, Dominik Lorenz, Axel Sauer, Frederic Boesel, Dustin Podell, Tim Dockhorn, Zion English, and Robin Rombach. Scaling rectified flow transformers for high-resolution image synthesis. In *Forty-first International Conference on Machine Learning*, 2024. 5
- [16] Martin Ester, Hans-Peter Kriegel, Jörg Sander, and Xiaowei Xu. A Density-Based Algorithm for Discovering Clusters in Large Spatial Databases with Noise. In *Second International Conference on Knowledge Discovery and Data Mining (KDD'96). Proceedings of a conference held August 2-4*, pages 226–331, 1996. 5
- [17] Shengbang Fang, Tai D Nguyen, and Matthew c Stamm. Open set synthetic image source attribution. In *34th British Machine Vision Conference 2023, BMVC 2023, Aberdeen, UK, November 20-24, 2023*. BMVA, 2023. 2, 5, 6
- [18] Joel Frank, Thorsten Eisenhofer, Lea Schönherr, Asja Fischer, Dorothea Kolossa, and Thorsten Holz. Leveraging frequency analysis for deep fake image recognition. In *International conference on machine learning*, pages 3247–3258. PMLR, 2020. 1
- [19] Tero Karras, Timo Aila, Samuli Laine, and Jaakko Lehtinen. Progressive growing of GANs for improved quality, stability, and variation. In *International Conference on Learning Representations*, 2018. 5
- [20] Tero Karras, Samuli Laine, and Timo Aila. A style-based generator architecture for generative adversarial networks. In *Proceedings of the IEEE/CVF conference on computer vision and pattern recognition*, pages 4401–4410, 2019. 5
- [21] Tero Karras, Samuli Laine, Miika Aittala, Janne Hellsten, Jaakko Lehtinen, and Timo Aila. Analyzing and improving the image quality of stylegan. In *Proceedings of the IEEE/CVF conference on computer vision and pattern recognition*, pages 8110–8119, 2020.
- [22] Tero Karras, Miika Aittala, Samuli Laine, Erik Härkönen, Janne Hellsten, Jaakko Lehtinen, and Timo Aila. Alias-free generative adversarial networks. *Advances in neural information processing systems*, 34:852–863, 2021. 5
- [23] Yun Liu, Zuliang Wan, Xiaohua Yin, Guanghui Yue, Aiping Tan, and Zhi Zheng. Detection of gan generated image using color gradient representation. *Journal of Visual Communication and Image Representation*, 95:103876, 2023. 2
- [24] I Loshchilov. Decoupled weight decay regularization. *arXiv preprint arXiv:1711.05101*, 2017. 5
- [25] Jan Lukas, Jessica Fridrich, and Miroslav Goljan. Digital camera identification from sensor pattern noise. *IEEE Transactions on Information Forensics and Security*, 1(2): 205–214, 2006. 2
- [26] Francesco Marra, Diego Gagnaniello, Davide Cozzolino, and Luisa Verdoliva. Detection of gan-generated fake images over social networks. In *2018 IEEE conference on multimedia information processing and retrieval (MIPR)*, pages 384–389. IEEE, 2018. 1, 2
- [27] Francesco Marra, Diego Gagnaniello, Luisa Verdoliva, and Giovanni Poggi. Do gans leave artificial fingerprints? In *2019 IEEE conference on multimedia information processing and retrieval (MIPR)*, pages 506–511. IEEE, 2019. 2

- [28] Francesco Marra, Cristiano Saltori, Giulia Boato, and Luisa Verdoliva. Incremental learning for the detection and classification of gan-generated images. In *2019 IEEE international workshop on information forensics and security (WIFS)*, pages 1–6. IEEE, 2019. 2
- [29] G. McLachlan and K. Basford. *Mixture Models: Inference and Applications to Clustering*. 1988. 5
- [30] Midjourney. Midjourney. <https://www.midjourney.com/home>. Accessed: March 7, 2025. 5
- [31] Lakshmanan Nataraj, Tajuddin Manhar Mohammed, Shivkumar Chandrasekaran, Arjuna Flenner, Jawadul H. Bappy, Amit K. Roy-Chowdhury, and B. S. Manjunath. Detecting gan generated fake images using co-occurrence matrices. *Electronic Imaging*, 2019. 2
- [32] Tai Nguyen, Aref Azizpour, and Matthew C. Stamm. Forensic self-descriptions are all you need for zero-shot detection, open-set source attribution, and clustering of ai-generated images. In *Proceedings of the IEEE/CVF Conference on Computer Vision and Pattern Recognition*, 2025. 1, 2, 3, 6
- [33] Utkarsh Ojha, Yuheng Li, and Yong Jae Lee. Towards universal fake image detectors that generalize across generative models. In *Proceedings of the IEEE/CVF Conference on Computer Vision and Pattern Recognition (CVPR)*, pages 24480–24489, 2023. 1, 6
- [34] Dustin Podell, Zion English, Kyle Lacey, Andreas Blattmann, Tim Dockhorn, Jonas Müller, Joe Penna, and Robin Rombach. Sdxl: Improving latent diffusion models for high-resolution image synthesis. *arXiv preprint arXiv:2307.01952*, 2023. 5
- [35] Jonas Ricker, Denis Lukovnikov, and Asja Fischer. Aeroblade: Training-free detection of latent diffusion images using autoencoder reconstruction error. In *Proceedings of the IEEE/CVF Conference on Computer Vision and Pattern Recognition (CVPR)*, pages 9130–9140, 2024. 1
- [36] Robin Rombach, Andreas Blattmann, Dominik Lorenz, Patrick Esser, and Björn Ommer. High-resolution image synthesis with latent diffusion models. In *Proceedings of the IEEE/CVF conference on computer vision and pattern recognition*, pages 10684–10695, 2022. 5
- [37] Olga Russakovsky, Jia Deng, Hao Su, Jonathan Krause, Sanjeev Satheesh, Sean Ma, Zhiheng Huang, Andrej Karpathy, Aditya Khosla, Michael Bernstein, Alexander C. Berg, and Li Fei-Fei. ImageNet Large Scale Visual Recognition Challenge. *International Journal of Computer Vision (IJCV)*, 115(3):211–252, 2015. 5
- [38] Zeyang Sha, Zheng Li, Ning Yu, and Yang Zhang. De-fake: Detection and attribution of fake images generated by text-to-image generation models. In *Proceedings of the 2023 ACM SIGSAC Conference on Computer and Communications Security*, page 3418–3432, New York, NY, USA, 2023. Association for Computing Machinery. 1
- [39] Sergey Sinitisa and Ohad Fried. Deep image fingerprint: Towards low budget synthetic image detection and model lineage analysis. In *Proceedings of the IEEE/CVF Winter Conference on Applications of Computer Vision*, pages 4067–4076, 2024. 1, 2
- [40] Chuangchuang Tan, Yao Zhao, Shikui Wei, Guanghua Gu, and Yunchao Wei. Learning on gradients: Generalized artifacts representation for gan-generated images detection. In *Proceedings of the IEEE/CVF Conference on Computer Vision and Pattern Recognition (CVPR)*, pages 12105–12114, 2023. 1
- [41] Chuangchuang Tan, Yao Zhao, Shikui Wei, Guanghua Gu, Ping Liu, and Yunchao Wei. Rethinking the up-sampling operations in cnn-based generative network for generalizable deepfake detection. In *Proceedings of the IEEE/CVF Conference on Computer Vision and Pattern Recognition (CVPR)*, pages 28130–28139, 2024. 1, 6
- [42] Diangarti Tariang, Riccardo Corvi, Davide Cozzolino, Giovanni Poggi, Koki Nagano, and Luisa Verdoliva. Synthetic image verification in the era of generative artificial intelligence: What works and what isn’t there yet. *IEEE Security & Privacy*, 22(3):37–49, 2024. 2
- [43] Laurens van der Maaten and Geoffrey Hinton. Visualizing data using t-sne. *Journal of Machine Learning Research*, 9(86):2579–2605, 2008. 4
- [44] Sheng-Yu Wang, Oliver Wang, Richard Zhang, Andrew Owens, and Alexei A. Efros. Cnn-generated images are surprisingly easy to spot... for now. In *Proceedings of the IEEE/CVF Conference on Computer Vision and Pattern Recognition (CVPR)*, 2020. 1, 2, 6
- [45] Tianyun Yang, Danding Wang, Fan Tang, Xinying Zhao, Juan Cao, and Sheng Tang. Progressive open space expansion for open-set model attribution. In *Proceedings of the IEEE/CVF Conference on Computer Vision and Pattern Recognition*, pages 15856–15865, 2023. 2, 6
- [46] Ning Yu, Larry S. Davis, and Mario Fritz. Attributing fake images to gans: Learning and analyzing gan fingerprints. In *Proceedings of the IEEE/CVF International Conference on Computer Vision (ICCV)*, 2019. 2
- [47] Xu Zhang, Svebor Karaman, and Shih-Fu Chang. Detecting and simulating artifacts in gan fake images. In *2019 IEEE International Workshop on Information Forensics and Security (WIFS)*, pages 1–6, 2019. 2

Autonomous and Self-Adapting System for Synthetic Media Detection and Attribution

Supplementary Material

Page	Appendix	Title
1	A	Implementation Details
1	B	Datasets

A. Implementation Details

Embedding Space. Following Sec. 4.1, we optimized our embedding space loss function using the AdamW optimizer with a learning rate of 10^{-4} and a weight decay of 0.01 for 50 epochs at each update step. We set the mini-batch size to 256 and created triplets using the 64 hardest positive samples and 64 hardest negative samples per anchor, resulting in 4096 pairs per anchor. An early stopping mechanism was employed to prevent overfitting. A balance factor of $\lambda = 1.0$ yielded the best performance.

Open-Set Source Attribution & Detection. To model the distribution of embeddings, we utilized a set of GMMs with 5 components and full covariance matrices. The acceptance confidence threshold τ_{reject} was chosen to maximize the difference $\text{TPR} - \text{FPR}$, where TPR is the true-positive rate of rejection of unknown samples, and FPR is the false-positive rate. These were measured using the validation set, $\mathcal{D}_V^{(\ell)}$, ensuring a high correct acceptance rate while keeping the incorrect acceptance rate low.

Clustering & Candidate Proposition. We selected DBSCAN as our unsupervised clustering algorithm because it does not require prior knowledge of the number of clusters and effectively detects outliers, thereby yielding purer clusters. We fixed the minimum samples parameter at 7 and searched for an epsilon value between 5 and 20 over 10 trials to find a satisfactory cluster at each step. Furthermore, we set the sufficiency threshold τ_c to 75 samples.

DBSCAN defines clusters as regions of high density separated by low-density areas. Two key parameters govern this process: epsilon and min_samples. A core sample is any point that has at least min_samples neighbors within a radius epsilon. Here, epsilon sets the size of the local neighborhood, while min_samples controls the minimum density required to form a cluster. Choosing a small epsilon results in many points being labeled as noise, whereas a large epsilon may merge distinct clusters. Similarly, increasing min_samples enhances noise tolerance but can reduce the number of clusters.

Dataset	Subset	# Samples
Known Sources	Training	750
	Validation	250
	Observation	750
	Test	250
Emerging Sources	Observation	750
	Test	250

Table 5. Dataset splits used in our experiments. The table shows the number of samples in each subset for both known and emerging sources.

B. Datasets

We used publicly available datasets containing both real and synthetic images. For real images, we employed ImageNet-1k. Our initial set of known synthetic sources was obtained from StyleGAN[1-3]. In addition, we considered emerging synthetic sources including Midjourney-v6, Adobe Firefly, Stable Diffusion (SD) 1.4, SD 1.5, SD 3.0, and SDXL. Synthetic images from these sources were collected from the datasets used in FSD, the OSSIA dataset, and the Synthbuster dataset.

For each source, the data were partitioned into disjoint subsets to serve different purposes. For the initially known sources, the data were divided into four subsets:

1. A **training set** used to train the initial embedding function f^0 and the open-set source attribution and detection model α , denoted as $\mathcal{D}_T^{(0)}$.
2. A **validation set** used to support model development, denoted as $\mathcal{D}_V^{(0)}$.
3. An **observation set** that simulates a continuous data stream.
4. A **test set** reserved for further analysis.

For emerging sources, the data were split into two disjoint subsets, as they are not used for initial training:

1. An **observation set** that is combined with the known sources' observation set. Samples from this combined set that are identified as unknown are stored in a buffer \mathcal{B} .
2. A **test set** reserved for further analysis.

Detailed statistics regarding the number of images in

each subset are provided in Tab. 5.